Tunneling Splitting of Energy Levels and Rotational Constants in the Vinyl Radical C_2H_3†

Gennady V. Mil'nikov,‡ Toshimasa Ishida,§ and Hiroki Nakamura*,‡

Department of Theoretical Studies, Institute for Molecular Science, Myodaiji, Okazaki 444-8585, Japan, and Fukui Institute for Fundamental Chemistry, Kyoto University 34-4, Takano-nishibirakicho, Kyoto 606-8103, Japan

Received: October 5, 2005; In Final Form: November 25, 2005

The instanton theory newly implemented by two of the authors (G.V.M. and H.N.) is applied to hydrogen tunneling transfer in a vinyl radical. The converged instanton trajectory is found on the CCSD(T)/aug-cc-pVTZ level of an ab initio potential energy surface. The calculated ground-state energy splitting agrees with the recent high-resolution experimental data within 3% of discrepancy. The semiclassical wave function is used to estimate the splitting of the principal rotational constants of the radical.

I. Introduction

The vinyl radical is an important intermediate in combustion chemistry, attracting much interest for many years.[1,2] Intensive works on its structure have been carried out by both theoreticians[3−7] and experimentalists.[8−15] In particular, Fessenden and Schuller observed a pair of doublets ascribed to an α proton in the CH group and two β protons in the CH_2 group.[10] They concluded that the absence of central $\alpha\beta$ and $\beta\alpha$ lines is due to the fast interconversion of the C−H bond between two minima and estimated the corresponding potential barrier height to be about 2 kcal/mol. Kanamori et al. reported the results obtained by the IR diode laser kinetic spectroscopy.[14] They observed the splitting of an absorption band around 900 cm^{-1} assigned to the out-of-plane CH_2 wagging motion. Although the tunneling splitting in the ground state Δ_0 cannot be directly estimated from their data, the authors derived the potential barrier height 1200 cm^{-1} from the analysis of rotational constants. Quite recently, Tanaka et al.[15] investigated this radical by millimeter-wave spectroscopy and reported a set of precise molecular constants. Among them, the ground-state tunneling splitting was found to be $\Delta_0 = 16\,272$ MHz (= 0.54 cm^{-1}). Using a one-dimensional (1D) double minimum model, they also estimated the barrier height as 1580 cm^{-1} as well as the tunneling splitting of the rotational constant.

The present work is addressed to a theoretical study of intramolecular tunneling hydrogen transfer in the vinyl radical. In addition to the tunneling splitting by the recently developed instanton theory,[16−19] we estimate the splitting of rotational constants with the use of the semiclassical wave function. Our method enables us to incorporate high-level ab initio quantum chemical calculations into the theory, which provide an effective practical recipe for studying tunneling processes in polyatomic systems. The final accuracy of the theoretical estimate mainly depends on the quality of electronic structure calculations. In the previous benchmark calculation of the malonaldehyde molecule,[18] the fully converged semiclassical result has been obtained at the CCSD/(aug-)cc-pVDZ computational level,[20,21] where the aug-cc-pVDZ set is used for oxygen atoms and the transferred hydrogen atom and the cc-pVDZ set for the other atoms. It was concluded, however, that the main origin of about 20% discrepancy in comparison with the experiment was due to the insufficient accuracy of the potential energy surface. By introducing the CCSD/(aug-)cc-pVTZ correction along the instanton tunneling path, we could reproduce the experiment within a few percent of accuracy. Accurate implementation of the instanton method requires the Hessian of the potential function to be evaluated. In the case of malonaldehyde, such potential data are not available at the highest CCSD/aug-cc-pVTZ level because of too much required CPU time and the accuracy of the theoretical estimate is not fully guaranteed. On the contrary, the vinyl radical supplies a good example that the full-scale semiclassical calculations at such a level can be accomplished.

This paper is organized as follows. In the next section, we slightly extend our instanton theory so that we can evaluate other physical quantities. We derive a simple formula to estimate the splitting of the expectation value of an arbitrary function of internal coordinates for the two lowest states. In section III, we apply our theory to the splitting of energy levels and principal rotational constants in the vinyl radical. Concluding remarks are presented in section IV.

II. Instanton Theory

In this section, we summarize the main equations of the instanton theory.[16,19] We also show that the semiclassical wave function enables us to estimate the splitting of an arbitrary physical quantity. In particular, we derive a practical formula for the splitting of rotational constants. The general Hamiltonian for a nonrotating ($J = 0$) N_a atomic molecule reads

$$\hat{H} = -\frac{\hbar^2}{2\sqrt{G}}\frac{\partial}{\partial q^i}\left(\sqrt{G}\, g^{ij}\frac{\partial}{\partial q^j}\right) + V(\mathbf{q}) \qquad (1)$$

where $\mathbf{q} = q^1, q^2, ..., q^N$ are $N = 3N_a - 6$ internal coordinates, $g^{ij}(\mathbf{q})$ is the Riemannian metric tensor for the internal motion, and G is the determinant of the full metric tensor for both internal and rotational degrees of freedom. It is assumed that the potential function $V(\mathbf{q})$ has two equivalent symmetric minima located at $\mathbf{q}_m$ and $\tilde{\mathbf{q}}_m$. Generally, the tunneling splitting of energy

† Part of the special issue "John C. Light Festschrift".

* To whom correspondence should be addressed. E-mail: nakamura@ims.ac.jp.

‡ Institute for Molecular Science.

§ Kyoto University.

10.1021/jp055667s CCC: $33.50 © 2006 American Chemical Society
Published on Web 01/05/2006

levels in a double well potential can be evaluated by means of the Herring formula[22] as a "flux" $\sim\int \Psi\nabla\Psi \, d\sigma$ through the symmetric dividing surface separating the two potential wells. In the instanton theory, the corresponding wave function is constructed in the semiclassical approximation as

$$\Psi = \exp\left(-\frac{W_0}{\hbar} - W_1\right) \tag{2}$$

where W_0 and W_1 are found from the Hamilton−Jacobi (HJ) and transport equations, respectively. In the present case, the HJ equation reads[16]

$$H\left(\mathbf{q}, \frac{\partial W_0}{\partial \mathbf{q}}\right) = 0 \tag{3}$$

where $H(\mathbf{q},\mathbf{p}) = (1/2)g^{ij}(\mathbf{q})p_ip_j - V(\mathbf{q})$ is the classical Hamiltonian with the upside down potential. Equation 3 can generally be solved by the method of characteristics. This gives $W_0(\mathbf{q})$ in the form of the action integral along the classical trajectories (characteristics) for the Hamiltonian $H(\mathbf{q},\mathbf{p})$. In particular, the family of characteristics originating from $\mathbf{q}_m$ or $\tilde{\mathbf{q}}_m$ gives the semiclassical wave function localized in the corresponding potential well. The calculation of the tunneling splitting is very much simplified due to the symmetry of the problem. It can be shown that within the limits of semiclassical accuracy the main contribution to the Herring formula comes from the vicinity of the so-called instanton trajectory $\mathbf{q}_0(\tau)$ which is nothing but the characteristic connecting the two potential minima $\mathbf{q}_m$ and $\tilde{\mathbf{q}}_m$.[16] This trajectory is generally defined up to an arbitrary time shift and can always be chosen to satisfy the conditions that $\mathbf{q}_0(-\infty) = \mathbf{q}_m$, $\mathbf{q}_0(\infty) = \tilde{\mathbf{q}}_m$, and $\mathbf{q}_0(\tau = 0)$ is the middle point of the instanton. Then, for the semiclassical wave function localized around $\mathbf{q}_m$, the solution of the HJ equation eq 3 in the vicinity of $\mathbf{q}_0(\tau)$ is given by[19]

$$W_0(\mathbf{q}) = \int_{-\infty}^{\tau} \mathbf{p}_0(\tau')\dot{\mathbf{q}}_0(\tau')\, d\tau' + \frac{1}{2}\Delta\mathbf{q}\tilde{\mathbf{A}}(\tau)\Delta\mathbf{q} + o((\Delta\mathbf{q}^2)) \tag{4}$$

Here, $\Delta\mathbf{q} \equiv \mathbf{q} - \mathbf{q}_0(\tau)$, $\mathbf{p}_0(\tau)$ is the conjugate momentum along the instanton trajectory, and the symmetric matrix $\tilde{\mathbf{A}}(\tau)$ satisfies the equation[16]

$$\frac{d}{d\tau}\tilde{\mathbf{A}} = -\mathrm{H}_{\mathbf{qq}} - \mathrm{H}_{\mathbf{qp}}\tilde{\mathbf{A}} - \tilde{\mathbf{A}}\mathrm{H}_{\mathbf{pq}} - \tilde{\mathbf{A}}\mathrm{H}_{\mathbf{pp}}\tilde{\mathbf{A}} \tag{5}$$

where $\mathrm{H}_{\mathbf{qq}}$, $\mathrm{H}_{\mathbf{qp}}$, ..., stand for the matrixes of the corresponding second derivatives of the classical Hamiltonian taken along $\mathbf{q}_0(\tau)$. Equation 5 is supplemented by the initial condition $(d/d\tau)A(-\infty) = 0$ which completely defines $\tilde{\mathbf{A}}(\tau)$. The time τ in eq 4 is understood as a function of coordinates $\tau(\mathbf{q})$ according to the relation[19]

$$(q^i - q_0^i(\tau))p_{0i}(\tau) = 0 \tag{6}$$

The second term $W_1(\mathbf{q})$ in the semiclassical expansion, eq 2, is easily found from the transport equation. In particular, for the ground state, it is given by[16]

$$W_1(\mathbf{q}) = \frac{1}{2}\int_{-\infty}^{\tau} (Tr(\mathbf{A}(\tau') - \mathbf{A}_m))\, d\tau' \tag{7}$$

where $Tr\mathbf{A} \equiv A_i^i = g^{ij}A_{ij}$, the matrix $\mathbf{A}$ differs from $\tilde{\mathbf{A}}$ by the curvature term $A_{ij} \equiv \tilde{A}_{ij} - p_{0k}\Gamma_{ij}^k$, and Γ_{ij}^k are the Christoffel symbols. Equations 2, 4, and 7 completely determine the semiclassical wave function, and the calculation of the tunneling splitting by the Herring formula is straightforward. We will show below that the explicit form of the wave function can also be used to estimate the tunneling splitting of rotational constants. Further details of the theory can be found in refs 16 and 19, and here we just collect the main results.

For the ground-state tunneling splitting, the general formula reads

$$\Delta_0 = B\exp\left(-\frac{S_0}{\hbar} - S_1\right) \tag{8}$$

where S_0 is the classical action along the instanton trajectory

$$S_1 = \int_{-\infty}^{0} d\tau\, [Tr(\mathbf{A} - \mathbf{A}_m)] \tag{9}$$

and

$$B = \sqrt{\frac{4\hbar G_b \det \mathbf{A}_m}{\pi G_m \det \mathbf{A}_b}}\frac{(\mathbf{p}_0^T\mathbf{g}\mathbf{p}_0)_b}{\sqrt{(\mathbf{p}_0^T\mathbf{A}^{-1}\mathbf{p}_0)_b}} \tag{10}$$

where indices m and b indicate that the corresponding quantities are taken at the potential minimum $\mathbf{q}_m$ and the barrier $\mathbf{q}_b \equiv \mathbf{q}(0)$, respectively.

Analysis of the excited state is more complicated, since the nodal structure of the wave function must be properly taken into account. It has been shown recently that for low vibrational excitations the invariant instanton theory can still be constructed.[19] In general, multidimensional systems, one can separate the excitation of the normal mode along the instanton trajectory (longitudinal mode) in the region of the potential minimum from the excitation of all the other $N - 1$ transversal modes. The former is especially simple, since the correction to the semiclassical solution due to the excitation is shown to be independent of all the transversal modes. Thus, the problem becomes essentially 1D, and the tunneling splitting for the first excited states is given by the simple formula[19]

$$\Delta_{n=1} = \Delta_{n=0}\frac{4V(0)}{\hbar\omega}\exp\left[2\int_{-\infty}^{0} d\tau\left(\omega - \frac{1}{2V}\frac{dV}{d\tau}\right)\right] \tag{11}$$

where ω is the corresponding longitudinal normal frequency and $V(\tau) \equiv V(\mathbf{q}_0(\tau))$.

The case of transversal excitations is more difficult. In addition to eq 5, one has to solve a complementary equation which describes the interaction between all the transversal modes and has the form

$$\dot{U}_k = \theta(\tau)U_k - [g^{ij}\tilde{A}_{ik} + \partial_k g^{ij}p_{0i}]U_j \tag{12}$$

where $\theta(\tau) = \sum_{ij}U^iU^jA_{ij}$ and, as before, all the quantities are taken on the instanton trajectory. The upper and lower indices indicate the contra- and co-variant vectors related by the metric tensor g^{ij} in the usual way. The vector $\mathbf{U}(\tau)$ characterizes the local direction of the node of semiclassical wave function. At the potential minimum, $\mathbf{U}(-\infty)$ coincides with one of the normal modes while $\theta(-\infty)$ is the corresponding normal frequency. $N - 1$ possible initial conditions for the transversal normal modes generates $N - 1$ independent solutions of eq 12 which describe the possible types of transversal excitation. For each normal mode γ, the tunneling splitting of the first excited state reads

$$\Delta_\gamma = \Delta_0\omega_\gamma\left(\mathbf{U}^T\left[\mathbf{A}^{-1} + \frac{(\mathbf{A}^{-1}\mathbf{p}_0)\otimes(\mathbf{p}_0^T\mathbf{A}^{-1})}{(\mathbf{p}_0^T\mathbf{A}^{-1}\mathbf{p}_0)}\right]\mathbf{U}\right)_b \exp(-\Delta S_1) \tag{13}$$

where ω_γ is the normal-mode frequency (excitation energy), and the extra exponential factor is given by

$$\Delta S_1 = 2\int_{-\infty}^{0} (\theta(\tau) - \omega_\gamma)\, d\tau \tag{14}$$

In the rest of this section, we discuss a more general problem of the semiclassical estimation of the expectation value of the physical quantity. For simplicity, we restrict our attention to the ground state with the wave function given explicitly by eqs 2, 4, and 7. The calculation of the matrix element generally requires the global wave function, while eq 4 gives only local behavior in close vicinity of the instanton trajectory. However, since our aim here is to estimate the difference between the expectation values of the two states of opposite symmetry in the tunneling doublet, the instanton theory can be used.

We consider the expectation values

$$\mathbf{B}^{\pm} \equiv \frac{1}{2}\langle \Psi^{\pm}|\mathbf{G}|\Psi^{\pm}\rangle \tag{15}$$

where $G^{kl}(\mathbf{q})$ ($k,l = 1, 2, 3$) is the rotational metric tensor, and $\Psi^{+}(\mathbf{q})$ and $\Psi^{-}(\mathbf{q})$ are the wave functions for symmetric and antisymmetric states in the ground-state doublet, respectively.

We introduce the functions $\Psi_{1,2} = (\Psi^{+} \pm \Psi^{-})/(2)^{1/2}$ localized in each potential well and rewrite eq 15 in the form

$$\mathbf{B}^{\pm} = \mathbf{M} \pm \mathbf{m} \tag{16}$$

with

$$\mathbf{M} = \frac{1}{4}(\langle \Psi_1|\mathbf{G}|\Psi_1\rangle + \langle \Psi_2|\mathbf{G}|\Psi_2\rangle) \tag{17}$$

and

$$\mathbf{m} = \frac{\langle \Psi_1|\mathbf{G}|\Psi_2\rangle}{2} \tag{18}$$

The rotational constants are defined as the eigenvalues of $\mathbf{B}^{\pm}$. By treating the second exponentially small term in eq 16 as a perturbation, we obtain the tunneling splitting of the rotational constants in the form

$$\Delta B_k = 2\mathbf{X}_k^T \mathbf{m} \mathbf{X}_k \tag{19}$$

where $\mathbf{X}_k$ ($k = 1, 2, 3$) are the eigenvectors of $\mathbf{M}$. Within the limits of semiclassical accuracy, the latter must be taken in zeroth-order approximation, that is, $\mathbf{M} = \mathbf{G}(\mathbf{q}_m)/2$. The problem therefore is reduced to calculating the exponentially small term, eq 18.

Let us consider a matrix element

$$I = \langle \Psi_1|f|\Psi_2\rangle \tag{20}$$

where $f(\mathbf{q})$ is an arbitrary function of coordinates which is assumed to possess appropriate symmetry. In the semiclassical approximation, the main contribution to the matrix element comes from the characteristic which is common for the two families of classical trajectories associated with the functions Ψ_1 and Ψ_2. This is nothing but the instanton trajectory, and the matrix element can be estimated from eqs 2, 4, and 7. The wave function $\Psi_2 = \exp(-W_0'/\hbar - W_1')$ is the semiclassical wave function localized in $\tilde{\mathbf{q}}_m$ and can be constructed in the same way as before. The principal exponent W_0', for instance, is explicitly given by

$$W_0'(\mathbf{q}) = \int_\tau^\infty p_{0i}(\tau')\dot{q}_0^i(\tau')\, d\tau' + \frac{1}{2}\tilde{A}_{ij}'(\tau)(q^i - q_0^i(\tau))(q^j - q_0^j(\tau)) + o((\Delta\mathbf{q}^2)) \tag{21}$$

where $\tilde{\mathbf{A}}'$ satisfies the same as eq 5 but with the initial condition specified at $\tau = \infty$.

Using this semiclassical form and neglecting the exponentially small contribution away from the instanton trajectory, we can estimate the matrix element as

$$I = N e^{-(S_0/\hbar)-S_1} \int \sqrt{G}\, d\mathbf{q}\, f(\mathbf{q}) \exp\left(-\frac{\Delta\mathbf{q}\mathbf{A}\Delta\mathbf{q}}{\hbar}\right) \tag{22}$$

where $\mathbf{A} = (\tilde{\mathbf{A}} + \tilde{\mathbf{A}}')/2$ and $N = (\det A_m/G_m(\hbar\pi)^N)^{1/2}$ is the normalization factor of the semiclassical wave function.[16] Equation 22 can be rewritten as a linear integral along the instanton path. Inserting the identity $1 = \int_{-\infty}^{\infty} d\tau\, \delta(\tau - \tau(\mathbf{q}))$ into the integrand and changing the order of integration, we obtain

$$I = N e^{-(S_0/\hbar)-S_1} \int d\tau \sqrt{G(\mathbf{q}_0(\tau))}\, f(\mathbf{q}_0(\tau)) \int d\mathbf{s}\, \delta\left(\frac{\partial\tau}{\partial\mathbf{q}}\mathbf{s}\right) \times \exp\left(-\frac{\mathbf{s}^T\mathbf{A}(\mathbf{q}_0(\tau))\mathbf{s}}{\hbar}\right) \tag{23}$$

up to the exponentially small terms. From eq 6, we find $\partial\tau/\partial\mathbf{q} = \mathbf{p}_0/(\mathbf{p}_0^T\mathbf{g}\mathbf{p}_0)$, and the integration in eq 23 gives

$$I = \sqrt{\frac{\det \mathbf{A}_m}{\hbar G_m \pi}}\, e^{-(S_0/\hbar)-S_1} \int d\tau \sqrt{\frac{G}{\det \mathbf{A}}} \frac{(\mathbf{p}_0^T\mathbf{g}\mathbf{p}_0)}{\sqrt{\mathbf{p}_0^T\mathbf{A}^{-1}\mathbf{p}_0}} f(\mathbf{q}_0(\tau)) \tag{24}$$

Although the above derivations are rather straightforward, one cannot expect high accuracy from eq 24. To see this, let us take $f(\mathbf{q}) = f_0 = \text{const}$. In this case, the above estimation gives $I = \propto f_0 e^{-(S_0/\hbar)-S_1}$, while the exact result is definitely $I = 0$ as follows from the definition of Ψ_1 and Ψ_2. In other words, the loss of exact orthogonality introduces the error comparable to the matrix element itself. The estimation can be, however, improved by rewriting eq 20 as

$$I = \langle \Psi_1|f - f(\mathbf{q}_r)|\Psi_2\rangle \tag{25}$$

where $\mathbf{q}_r$ is an arbitrary reference point. This modification does not affect the exact value of the matrix element, but in the semiclassical approximation, it corresponds to the change $f(\mathbf{q}_0(\tau)) \rightarrow f(\mathbf{q}_0(\tau)) - f(\mathbf{q}_r)$ in the integrand of eq 24. In the present calculations below, we take $\mathbf{q}_r = \mathbf{q}_b$, the symmetric midpoint of the instanton trajectory, which seems the only reasonable choice in the present problem.

III. Results

We numerate the atoms in the vinyl radical as shown in Figure 1. The body-fixed frame (BF) of reference is specified by imposing six conditions on the 15 BF Cartesian coordinates $\mathbf{r}_n = \sum_{i=1}^{3} x_{in}\mathbf{e}_i$ ($n = 1, 2, ..., 5$). The first three conditions fix the origin to the center of mass. The other three conditions specify the orientation of the BF axes ($\mathbf{e}_1$,$\mathbf{e}_2$,$\mathbf{e}_3$) in such a way that the "tunneling" H_5 lies in the ($\mathbf{e}_1$,$\mathbf{e}_2$) plane and $\mathbf{e}_1$ is directed along the line connecting the two hydrogen atoms in the CH_2 group. By the use of these conditions, the metric tensor for the rotation-

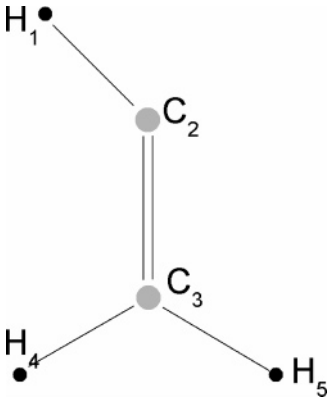

Figure 1. Vinyl radical.

free ($J = 0$) quantum Hamiltonian is constructed in the same way as in ref 18.

The instanton trajectory was calculated by the iterative variational method,[16] which enables one to incorporate the high-quality quantum chemical ab initio data directly, that is, without constructing a global potential energy function.[18] The method finds the instanton path in the analytical form

$$q_0^i(z,\{C\}) = \left[\frac{q_m^i + \tilde{q}_m^i}{2} + \frac{q_m^i - \tilde{q}_m^i}{2} z\right] + \sum_{n=1}^{N_b} C^{in}\varphi_n(z) \qquad (26)$$

where the parameter $z \in [-1{:}1]$ plays a role of the coordinate along the path.[16] The first term in eq 26 represents the straight line connecting the two minima and $\varphi_n(z)$ is a set of smooth basis functions under the condition $\varphi_n(\pm 1) = 0$. This reduces the problem to minimization of the classical action $S_0(\{C\})$ on the inverted potential as a function of $N \times N_b$ coefficients C^{in}. At each step of the iteration, the required ab initio information includes the values of the potential and its gradient and Hessian evaluated at some reference points along a trial instanton path. In the present calculations, we used 12 reference points at each step. The quantum chemical calculations were performed at the MP2/6-31G(d,p) level[23,24] and CCSD(T)/aug-cc-pVTZ level[21,25] of electronic structure theory. The gradients and Hessians required at each point were calculated analytically at the MP2 level and numerically at the CCSD(T) level using the Gaussian program.[26]

Table 1 shows a comparison of the normal-mode frequencies by the two methods (third and fourth columns). The instanton trajectory was first calculated at the ab initio MP2 level, where computations are cheap and analytical second derivatives are available. Starting from the straight line connecting the two potential minima as the initial trial path, full convergence was achieved after 10 iterations with 5 stable significant digits in the classical action guaranteed. By the use of this instanton trajectory, eq 5 was solved by the standard Runge−Kutta method and the tunneling splitting of the ground state Δ_0 was calculated from eq 8. At the ab initio MP2/6-31G(d,p) level, we obtained $\Delta_0 = 0.14$ cm^{-1} which is about four times smaller than the experimental value. This disparity is likely to be related to the insufficient accuracy of the potential data. In particular, the potential barrier along the instanton path at the MP2/6-31G-(d,p) level turns out to be as high as 2249 cm^{-1}. Our experience shows that one should not generally expect any accurate results from the simulations on the MP2 PES. At the same time, this preliminary step is necessary in order to reduce the numerical efforts at the CCSD(T)/aug-cc-pVTZ level. This is an important feature of our iterative method which enables us to use the obtained instanton path as the initial trial guess for the higher level of computations. The choice of the ab initio scheme at the preliminary stage is not important, and any numerically cheap method can be used. Due to the similarity of potential topology, usage of such a trial path reduces the number of iterations at the higher level and the calculation can be completed within a reasonable time effort. In the present case, only two extra iterations turn out to be enough to obtain three stable significant digits in the classical action at the CCSD(T)/aug-cc-pVTZ level of electronic structure calculations. The convergence of the iterative procedure is illustrated in Figure 2, which shows the projection of the instanton path onto the (XY) plane for the tunneling hydrogen atom. The paths numerated from 1 to 9 correspond to the successive steps of iteration using the MP2 ab initio calculations. As one can see from Figure 2, the ninth path and the path at the CCSD(T)/aug-cc-pVTZ level are essentially the same in shape and the main difference consists of the shift in the minimum positions. A similar behavior has been previously observed in malonaldehyde[18] and formic acid dimer.[27]

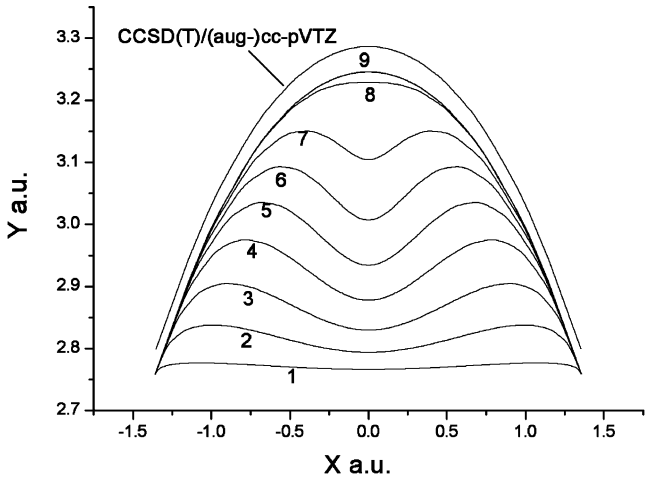

Figure 2. Iterative calculation of the instanton path. The labeled paths from 1 to 9 show gradual improvement of the instanton trajectory shape using the MP2/cc-pVDZ ab initio data. After switching to the CCSD-(T)/(aug-)cc-pVTZ ab initio method, only two more steps are required to achieve convergence and obtain the final result.

TABLE 1: Normal Frequencies (in cm^{-1}) and Corresponding Tunneling Splittings for the First Excited States

N	type of the motion	$\omega\gamma$ CCSD(T)/ aug-cc-pVTZ	$\omega\gamma$ MP2/ 6-31G(d,p)	Δ/Δ_0 CCSD(T)/ aug-cc-pVTZ	Δ/Δ_0 MP2/ 6-31G(d,p)
1	C_2H_1 rocking vibration	711	771.	36.0	41.1
2	wagging (out-of-plane)	813	996	2.20	1.76
3	wagging (out-of-plane)	923	1063	1.28	1.12
4	plane distortion	1062	1129	3.0	2.3
5	$H_4C_3H_5$ bending	1390	1465	1.7×10	1.5
6	C_2C_3 stretching	1632	1863	2×10^2	7×10
7	H_5C_3 stretching	3065	3203		
8	$H_1H_2H_3$ assym. bending	3171	3305		
9	C_2H_1 stretching	3238	3360		

TABLE 2: Tunneling Splitting of the Ground-State Energy Level and Rotational Constants

methods	classical barrier[a] (cm^{-1})	effective barrier[b] (cm^{-1})	Δ_0 (cm^{-1})	B (cm^{-1})	S_0 (au)	S_1	rotational constants (MHz) (average and difference)[c] A	B	C
MP2/6-31G(d,p)	2233	2249	0.14	2234	10.65	−0.98			
CCSD(T)/aug-cc-pVTZ	1761	1770	0.53	2023	9.37	−1.11	231 800	33 890	28 500
							227	10.2	1.1
experimental		1580[d,e]	0.54[d]				237 065[d]	32 480[d]	28 438[d]
							299[d]	2.74[d]	0.88[d]

[a] The difference between the saddle point and the minima (without zero point energy correction). [b] The barrier height along the instanton path. [c] Upper and lower are the average and difference of the constant, respectively. [d] Reference 15 (K. Tanaka et al.). [e] One-dimensional model is used.

TABLE 3: Barrier Height in the Vinyl Radical for Various ab Initio Methods

ab initio method	classical barrier (cm^{-1})	classical barrier (kcal/mol)	effective barrier[a] (cm^{-1})
MP2/6-31G(d,p)	2232.8	6.38	
MP2/aug-cc-pVDZ	2063.1	5.90	
MP2/aug-cc-pVTZ	1749.2	5.00	
MP2/aug-cc-pVQZ	1740.2	4.98	
CCSD/6-31G(d,p)	2224.2	6.36	
CCSD/aug-cc-pVDZ	2086.8	5.97	
CCSD/aug-cc-pVTZ	1805.5	5.16	
CCSD(T)/6-31G(d,p)	2209.7	6.32	
CCSD(T)/aug-cc-pVDZ	2058.5	5.89	
CCSD(T)/aug-cc-pVTZ	1761.3	5.04	1773.2
CCSD(T)/cc-pVQZ			1784.7
CCSD(T)/aug-cc-pVQZ			1768.1

[a] The energy difference between the middle point of the CCSD(T)/aug-cc-pVTZ instanton path and the minima.

At the CCSD(T)/aug-cc-pVTZ level, our theory gives the ground-state splitting as $\Delta_0 = 0.53\ cm^{-1}$ which almost perfectly reproduces the experimental value $\Delta_0 = 0.54\ cm^{-1}$ (see Table 2). In Table 2, we also show separately the three factors B, S_0, and S_1in eq 8. As one can see, the difference in Δ_0 between the two methods comes totally from the principal exponent S_0 and the other two factors are fairly close to each other. This also confirms the above surmise about the similarity in the potential topology for different ab initio methods. On the other hand, the principal exponent is mainly affected by the height of the potential barrier which in the case of CCSD(T)/aug-cc-pVTZ reduces to 1770 cm^{-1}. Note that there is almost 200 cm^{-1} difference from the estimate made by Tanaka et al.[15] which is probably due to the drawback of their 1D model.

It should be mentioned that from the theoretical viewpoint the accuracy of the instanton method is not very clear, since it is generally affected by both semiclassical approximation and the quality of the ab initio potential data. The accuracy of the instanton theory has been previously checked for simple 1- and 2D model systems. Recently, we have also calculated the tunnel splitting in spectrum of the realistic nonrotating ($J = 0$) HO_2 complex and found the agreement with the exact quantum data within a few percent.[16] On the other hand, inaccuracy in the potential energy surface can erroneously change the order of magnitude of the tunneling rate and the ab initio level is expected to be a more crucial factor. The full ab initio convergence test would imply a direct comparison with the results obtained for a larger basis for which the CCSD(T) scheme is prohibitively time-consuming. To provide an additional accuracy check, we have calculated the transition state energies for different, less refined schemes as well as the effected barrier height along the instanton path for CCSD(T)/cc-pVQZ and CCSD(T)/aug-cc-pVQZ ab initio levels. Table 3 shows that the CCSD(T) barrier heights are almost the same as the corresponding MP2 ones with 6-31G(d,p), aug-cc-pVDZ, and aug-cc-pVTZ basis sets. One can further see that the MP2/aug-cc-pVQZ barrier height 4.98 kcal/mol is very similar to 5.00 kcal/mol for MP2/aug-cc-pVTZ. This tendency suggests that the CCSD(T)/aug-cc-pVQZ barrier height is close to the one for CCSD(T)/aug-cc-pVTZ and this basis is large enough to provide a converged result. The same conclusion follows from the values of the effective barrier V_0 shown in the last column of Table 3. Assuming $S_0 \propto (V_0)^{1/2}$, we can estimate the accuracy of the classical action $\delta S_0 < 0.03$ which corresponds ~3% error in the tunnel splitting.

Using the results obtained at the ab initio CCSD(T)/aug-cc-pVTZ level, we estimated the splitting of rotational constants by the method explained at the end of the preceding section. These results are also presented in Table 2. Diagonalization of the rotational metrics at the potential minimum gives the average value of three rotational constants and the corresponding eigenvectors $\mathbf{X}_k$ (see eq 19). Then, the splitting of rotational constants is estimated from eqs 18−20 and 24. One can see from Table 2 that the semiclassical estimate reproduces the rotational constants and their splittings qualitatively but the absolute values are not very good compared to Δ_0, as expected.

Finally, we applied the instanton theory of low excited states to nine possible normal-mode excitations. The results for the CCSD(T)/aug-cc-pVTZ and MP2/6-31G(d,p) methods are shown in the fifth and sixth columns of Table 1. In the present case, the longitudinal normal mode is the lowest one which corresponds to the rocking vibration of the tunneling hydrogen atom. This has also been checked numerically by calculating the projection $(d\mathbf{q}_0/d\tau)\mathbf{n} \approx 0.99|(d\mathbf{q}_0/d\tau)||\mathbf{n}|$ at the potential minimum where $\mathbf{n}$ is the corresponding direction for the first normal mode. For this rocking mode excitation, the instanton theory predicts about 40 times growth of the tunneling splitting and both of the ab initio methods give similar results. The situation changes in the case of transversal mode excitation. For low-energy modes, one observes a moderate growth of the tunnel splitting but the result is more sensitive to the details of the potential energy surface compared to the rocking mode. For the fifth and sixth vibrational mode, one can expect a strong promotion effect and accurate evaluation of the potential energy surface is required. A similar effect has been found before in other systems, and this is explained by different behaviors of the solution of eq 12 for low and high excitations. In Figure 3, we depict the effective frequency θ in eq 12 as a function of the parameter z. The point $z = -1$ corresponds to $\tau = -\infty$, that is, the potential minimum. For all the transversal modes, the effective frequency monotonically decreases, which leads to the negative exponential factor ΔS_1 in eq 14. For higher frequency modes, the curve of θ is steeper, indicating a strong interaction with the lower frequency vibrations. In this region, the exponential factor in eq 13 becomes dominant but more sensitive to the ab initio method. Finally, for the last three modes ($N = 7-9$ in Table 2), ΔS_1 becomes comparable with the principal exponential factor S_0 which indicates a breakdown of the semiclassical approximation. This is not surprising since the

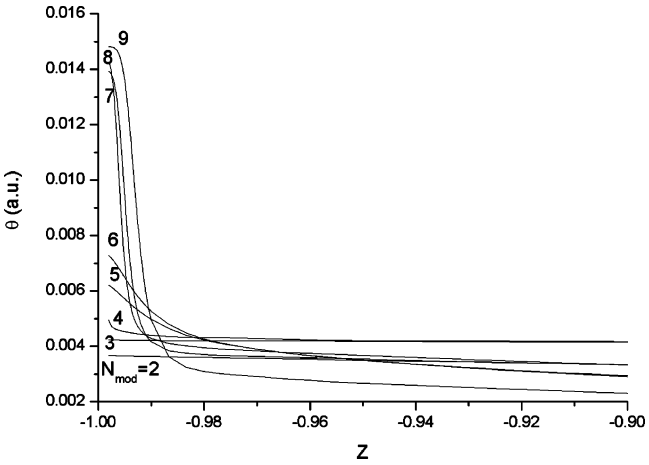

Figure 3. Effective frequency $\theta(z)$ in the integrand of eq 14 for eight transversal excitations. The steep decrease of $\theta(z)$ in the case of high excitations indicates a strong interaction with low modes. This leads to the breakdown of the theory for modes 7−9.

main assumption of this theory is the localization of the wave function which remains harmonic in the close vicinity of the potential minimum. For modes $N > 6$, the excitation energy exceeds the potential barrier height and this simple picture becomes incorrect.

IV. Concluding Remarks

In this work, we applied our instanton theory to the tunneling splitting in the vinyl radical. The instanton method is a powerful tool to analyze the hydrogen tunneling in real polyatomic systems, as it enables one to incorporate high-quality ab initio potential data with reasonable computational effort. In the present work, the instanton trajectory was initially found by the iterative variational method on the MP2/6-31G(d,p) ab initio potential after 10 iterations with the accuracy of 5 significant digits in the classical action. This result was further used as a initial trial path for the high-quality CCSD(T) ab initio method with a large aug-cc-pVTZ basis set. Thanks to the preliminary MP2/6-31G(d,p) calculations, only two extra iterations were enough to achieve the convergence on the CCSD(T)/aug-cc-pVTZ potential. The final tunneling splitting $\Delta_0 = 0.53\ cm^{-1}$ is in perfect agreement with the precise millimeter-wave spectroscopy value $\Delta_0 = 0.54\ cm^{-1}$ reported by Tanaka et al.[15] This confirms the accuracy of the semiclassical instanton method and also indicates that the presently used CCSD(T)/aug-cc-pVTZ method is good enough for a theoretical description of the single hydrogen transfer processes. From the present calculations, we extracted the effective potential barrier as 1770 cm^{-1} and also estimated the tunneling splitting of the principal rotational constants in the radical. The latter are also found to be close to the experimental data by Tanaka et al.[15]

Acknowledgment. This work was supported by a Grant-in-Aid for Specially Promoted Research on "Studies of Nonadiabatic Chemical Dynamics based on the Zhu−Nakamura Theory" from MEXT, Japan. We also thank Professor K. Tanaka for drawing our attention to this problem and useful discussions.

References and Notes

(1) Gardiner, W. C., Jr., Ed. *Combustion Chemistry*; Springer: New York, 1984.
(2) Okabe, H. *Photochemistry in Small Molecules*; Wiley: New York, 1978.
(3) Dupuis, M.; Wendoloski, J. J. *J. Chem. Phys.* **1984**, *80*, 5696.
(4) Boyd, S. L.; Boyd, R. J.; Barclay, C. L. R. *J. Am. Chem. Soc.* **1990**, *112*, 5724.
(5) Wang, J. H.; Chang, H. C.; Chen, Y. T. *Chem. Phys.* **1996**, *206*, 43.
(6) Peterson, K. A.; Dunning, T. H., Jr. *J. Chem. Phys.* **1997**, *106*, 4119.
(7) Perera, S. A.; Salemi, L. M.; Bartlett, R. J. *J. Chem. Phys.* **1997**, *106*, 4061.
(8) Cochran, E. L.; Adrian, F. J.; Bowers, V. A. *J. Chem. Phys.* **1964**, *40*, 213.
(9) Kasai, P. H. *J. Am. Chem. Soc.* **1972**, *94*, 5950.
(10) Fessenden, R. W.; Schuler, R. H. *J. Chem. Phys.* **1963**, *39*, 2147.
(11) Kim, E.; Yamamoto, S. *J. Chem. Phys.* **2002**, *116*, 10713.
(12) Tonokura, K.; Marui, S.; Koshi, M. *Chem. Phys. Lett.* **1999**, *313*, 771.
(13) Fahr, A.; Hassanzadeh, P.; Atkinson, D. B. *Chem. Phys.* **1998**, *236*, 43.
(14) Kanamori, H.; Endo, Y.; Hirota, E. *J. Chem. Phys.* **1990**, *92*, 197.
(15) Tanaka, K.; Toshimitsu, M.; Harada, K.; Tanaka, T. *J. Chem. Phys.* **2004**, *120*, 3604.
(16) Mil'nikov, G. V.; Nakamura, H. *J. Chem. Phys.* **2001**, *115*, 6881.
(17) Mil'nikov, G. V.; Yagi, K.; Taketsugu, T.; Nakamura, H.; Hirao, K. *J. Chem. Phys.* **2003**, *119*, 10.
(18) Mil'nikov, G. V.; Yagi, K.; Taketsugu, T.; Nakamura, H.; Hirao, K. *J. Chem. Phys.* **2004**, *120*, 5036.
(19) Mil'nikov, G. V.; Nakamura, H. *J. Chem. Phys.* **2005**, *122*, 124311.
(20) Cizek, J. *Adv. Chem. Phys.* **1969**, *14*, 35. Purvis, G. D.; Bartlett, R. J. *J. Chem. Phys.* **1982**, *76*, 1910. Scuseria, G. E.; Janssen, C. L.; Schaefer, H. F. *J. Chem. Phys.* **1998**, *89*, 7382. Scuseria, G. E.; Schaefer, H. F. *J. Chem. Phys.* **1989**, *90*, 3700.
(21) Dunning, T. H. *J. Chem. Phys.* **1989**, *90*, 1007.
(22) Herring, C. *Rev. Mod. Phys.* **1962**, *34*, 631.
(23) Moller, C.; Plesset, M. S. *Phys. Rev.* **1934**, *46*, 618. Head-Gordon, M.; Pople, J. A.; Frisch, M. J. *Chem. Phys. Lett.* **1988**, *153*, 503.
(24) Hehre, W. J.; Ditchfield, R.; Pople, J. A. *J. Chem. Phys.* **1972**, *56*, 2257.
(25) Pople, J. A.; Head-Gordon, M.; Raghavachari, K. *J. Chem. Phys.* **1987**, *87*, 5968.
(26) Frisch, M. J.; Trucks, G. W.; Schlegel, H. B.; Scuseria, G. E.; Robb, M. A.; Cheeseman, J. R.; Montgomery, J. A., Jr.; Vreven, T.; Kudin, K. N.; Burant, J. C.; Millam, J. M.; Iyengar, S. S.; Tomasi, J.; Barone, V.; Mennucci, B.; Cossi, M.; Scalmani, G.; Rega, N.; Petersson, G. A.; Nakatsuji, H.; Hada, M.; Ehara, M.; Toyota, K.; Fukuda, R.; Hasegawa, J.; Ishida, M.; Nakajima, T.; Honda, Y.; Kitao, O.; Nakai, H.; Klene, M.; Li, X.; Knox, J. E.; Hratchian, H. P.; Cross, J. B.; Bakken, V.; Adamo, C.; Jaramillo, J.; Gomperts, R.; Stratmann, R. E.; Yazyev, O.; Austin, A. J.; Cammi, R.; Pomelli, C.; Ochterski, J. W.; Ayala, P. Y.; Morokuma, K.; Voth, G. A.; Salvador, P.; Dannenberg, J. J.; Zakrzewski, V. G.; Dapprich, S.; Daniels, A. D.; Strain, M. C.; Farkas, O.; Malick, D. K.; Rabuck, A. D.; Raghavachari, K.; Foresman, J. B.; Ortiz, J. V.; Cui, Q.; Baboul, A. G.; Clifford, S.; Cioslowski, J.; Stefanov, B. B.; Liu, G.; Liashenko, A.; Piskorz, P.; Komaromi, I.; Martin, R. L.; Fox, D. J.; Keith, T.; Al-Laham, M. A.; Peng, C. Y.; Nanayakkara, A.; Challacombe, M.; Gill, P. M. W.; Johnson, B.; Chen, W.; Wong, M. W.; Gonzalez, C.; Pople, J. A. *Gaussian 03*, revision B.05; Gaussian, Inc.: Wallingford, CT, 2004.
(27) Mil'nikov, G. V.; Kuhn O.; Nakamura, H. *J. Chem. Phys.* **2005**, *123*, 074308.